Rapid Communications

Searching for muonic forces with the ATLAS detector

Iftah Galon [1,*] Enrique Kajamovitz,[2,†] David Shih [1,‡] Yotam Soreq [3,2,§] and Shlomit Tarem[2,‖]

[1]*New High Energy Theory Center, Dept. of Physics and Astronomy, Rutgers University, Piscataway, New Jersey 08854 USA*
[2]*Physics Department, Technion - Israel Institute of Technology, Haifa 3200003, Israel*
[3]*Theoretical Physics Department, The European Organization for Nuclear Research, CH-1211 Geneva 23, Switzerland*

The LHC copiously produces muons via different processes, and the muon sample will be large at the high-luminosity LHC (HL-LHC). In this work we propose to leverage this large muon sample and utilize the HL-LHC as a muon fixed-target experiment, with the ATLAS calorimeter as the target. We consider a novel analysis for the ATLAS detector, which takes advantage of the two independent muon momentum measurements by the inner detector and the muon system. We show that a comparison of the two measurements, before and after the calorimeters, can probe new force carriers that are coupled to muons and escape detection. The proposed analysis, based on muon samples from W and Z decays only, has a comparable reach to other proposals. In particular, it can explore the part of parameter space that could explain the muon $g-2$ anomaly.

I. INTRODUCTION

The Standard Model (SM) of particle physics has been successful in describing the known elementary particles and their interactions and is directly tested by experiments up to the TeV scale. Nevertheless, the SM is not a complete description of nature, and should be augmented by new physics (NP) degrees of freedom which account for neutrino oscillations, dark matter (DM), and the matter/antimatter asymmetry of the Universe.

One possible manifestation of NP are new particles with masses in the MeV-to-GeV range and suppressed couplings to the SM. Such new particles could be part or all of DM, or act as mediators to a dark sector. Muonic force carrier (MFC) mediators, X, are particularly interesting. These mediators have flavor-specific couplings [1–4], couple to the SM only through muons and may decay predominantly to DM. MFCs potentially explain inconsistencies in low-energy observations such as the anomalous magnetic dipole moment of the muon [5,6], and the possible anomaly in the measurement of the proton radius in muonic hydrogen [7,8].

Existing constraints on the existence of dark sector mediators are predominantly derived from beam-dump, fixed-target, or collider experiments [9–11]. The constraints are weaker for models where the mediator couplings to electrons or protons are suppressed. Specifically, MFC mediators are only weakly constrained [2]. Models where $m_X > 2m_\mu$ and X dominantly decays back to $\mu^+\mu^-$ are constrained by the *BABAR* analysis [12]. Data from rare B decays also constrain MFC mediators [13], but with larger model dependency.

Recent studies suggest that MFCs could be searched for in muon-fixed-target experiments [2,14–16], in kaon decays at the NA62 experiment [17] or in Belle II [18]. MFC production in muon-target interactions would register as a momentum difference between the incoming and outgoing muons which is not accounted for by the energy deposition in the (instrumented) target. Such dedicated apparatuses may be available at CERN by running the NA64 experiment with a muon beam [2,19], and at FermiLab, by leveraging the muon beam line of the Muon $(g-2)$ experiment [20], and constructing the M^3 apparatus [15].

In this article, we propose to utilize the ATLAS detector as a muon fixed-target experiment, which is sensitive to the missing muon momentum signature and therefore probes MFCs. The calorimeters serve as an instrumented target, and the inner detector (ID), and muon system (MS) provide independent muon momentum measurements before and after the target, as illustrated in Fig. 1. It is important that in ATLAS there is no uninstrumented material between the calorimeter and the MS. This ensures that an accurate measurement of the missing muon momentum signature is possible.

*iftah.galon@physics.rutgers.edu
†enrique@physics.technion.ac.il
‡dshih@physics.rutgers.edu
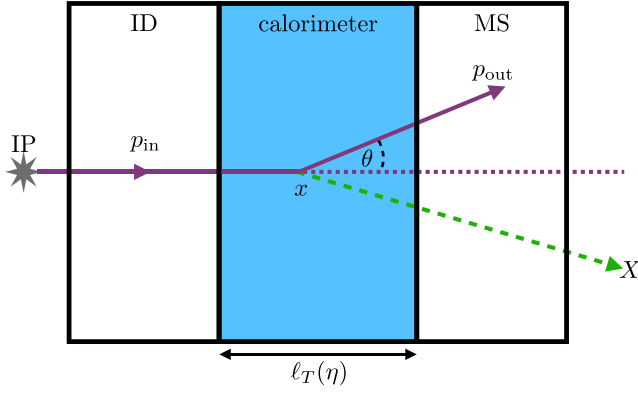§yotam.soreq@cern.ch
‖shlomit.tarem@cern.ch

FIG. 1. An illustration of the proposed measurement—the ATLAS detector as muon fixed-target experiment.

Using muons from Z and W decays, in total $\mathcal{O}(10^{10})$ muons on target at the high-luminosity LHC (HL-LHC), we estimate that the proposed analysis is sensitive to MFC masses in the MeV-GeV range with couplings as low as $g_X \sim 10^{-4}\text{--}10^{-3}$. This MFC parameter space includes the region which is relevant to account for the $(g-2)_\mu$ anomaly and is comparable to other proposals such as M^3 phase 1 and NA62. The fact that our proposal is based on an existing experiment, with well-known and excellent performances, is a big advantage compared to other recent proposals which are much more hypothetical in nature.

Our idea to use the ATLAS detector as a muon fixed-target experiment is a novel one, and we believe it can be extended to probe other new physics scenarios based on the same principles. This analysis can also be adopted by future high energy colliders and thus it can play a role in future detector design.

II. BENCHMARK MODELS

We use as MFC benchmarks scalar or vector mediators, i.e., $X = S$ or V [2,15–18]. The effective interaction Lagrangians are given by

$$\mathcal{L}_V = g_V V_\alpha \bar{\mu} \gamma^\alpha \mu, \qquad \mathcal{L}_S = g_S S \bar{\mu} \mu, \qquad (1)$$

where we have omitted the mass and kinetic terms. We assume that X is a mediator to a dark sector which predominantly decays into undetected particles, i.e., implicitly assume large couplings of X to sufficiently light dark sector constituents. Alternatively, X could be sufficiently long lived so as to escape detection.

The effective interaction in Eq. (1) can be UV completed. For example, the vector interaction may arise in a broken gauged $L_\mu - L_\tau$ gauge theory [21]. The scalar interaction can be a result of interactions with heavy leptons, which are integrated out [17].

The simplified models in Eq. (1) are subject to existing constraints depending on their UV completion. Here we consider (a) the muon magnetic moments [5,6], $(g-2)_\mu$;

and (b) from CHARM-II μ trident [22,23]. The bound from $(g-2)_\mu$ can be avoided in models where different contributions to the loop cancel each other, for example, scalar and vector against pseudoscalar and axial vector, e.g., see [24]. The μ-trident bound is valid only for vector mediators with left-handed coupling to the muon.

III. ATLAS AS A MUON FIXED-TARGET EXPERIMENT

Muons produced at the ATLAS interaction point (IP) traverse the entire detector, leaving signals in the ID, calorimeters, and MS. ATLAS muon reconstruction [25] is first performed independently in the ID and MS, with each detector subsystem providing muon spatial location and transverse-momentum (p_T) measurements. Subsequently the ID and MS information is combined with the calorimeter measurement to form the muon tracks which are used in physics analyses.

ATLAS defines four muon types, according to the details of the combination procedure, of which two are relevant for this work

 (i) A combined (CB) muon track is formed from independent tracks in the ID and MS, with a global refit that uses the hits from both subdetectors.
 (ii) Extrapolated (ME) muons have trajectories reconstructed based only on the MS track and a loose requirement on compatibility with originating from the IP. The muon track parameters are defined at the IP, and take into account the muon energy loss estimation, $p_{ME} \approx p_{MS} + E_{cal}$. The latter estimate combines the calorimeter measurement with a detailed analytic parametrization of the average energy loss, a method which yields a precision of $\sim$30 MeV for 50 GeV muons. ME muons are ideal candidates for an ATLAS search of the MFC signal.

MFC production in the muon-target interaction manifests as

$$p_{MS} + E_{cal} - p_{ID} < 0; \qquad (2)$$

a difference between p_{ID} and p_{MS} that is not compensated by E_{cal}. We define an observable which combines the ID momentum measurement, p_{ID}, with, p_{ME}, the reconstructed momentum of an ME type muon,

$$\rho \equiv \frac{p_{ME} - p_{ID}}{p_{ID}} \approx \frac{p_{out} - p_{in}}{p_{in}}, \qquad (3)$$

where, up to resolution effects, we identify the incoming (outgoing) muon momentum with respect to the target, $p_{in}(p_{out})$, with $p_{ID}(p_{ME})$.

The tag-and-probe method with $Z \to \mu\mu$, where one muon is reconstructed as a CB muon (tag) and the second may be a ME muon (probe), provides a high-purity muon sample [25] with loose selection on the probe muon that can be used to search for MFCs. We foresee that with careful analysis it will be possible to also use $W \to \mu\nu$ decays.

IV. SENSITIVITY ESTIMATION

Next, we estimate the sensitivity of the proposed analysis to probe MFCs, which are described by the interactions in Eq. (1). Throughout we will normalize our projections to the expected integrated luminosity of the HL-LHC, $\mathcal{L}_{\mathrm{LHC}}^{\mathrm{int}} = 3~\mathrm{ab}^{-1}$.

A. Muon-target luminosity and MFC production rate

For minimally ionizing particles such as muons, the fixed-target effective luminosity is given by

$$\mathcal{L}_{\mathrm{FT}}^{\mathrm{int}} = N_\mu \frac{\rho_T}{A m_0} \Delta x$$
$$= \left(\frac{\mathcal{L}_{\mathrm{LHC}}^{\mathrm{int}}}{3~\mathrm{ab}^{-1}} \right) \left(\frac{\sigma_{\mathrm{prod}}^{\mathrm{fid}}}{\mathrm{nb}} \right) \left(\frac{63}{A} \right)$$
$$\times \left(\frac{\rho_T}{8.96~\mathrm{g/cm^3}} \right) \left(\frac{\Delta x}{253~\mathrm{cm}} \right) 65~\mathrm{nb}^{-1}, \quad (4)$$

where we have treated the ATLAS calorimeter[1] as a thin target, and assumed a single material composition,[2] with density ρ_T, mass number A, length Δx and $N_\mu = \mathcal{L}_{\mathrm{LHC}}^{\mathrm{int}} \sigma_{\mathrm{prod}}^{\mathrm{fid}}$ incoming muons. Here, $m_0 = 1.661 \times 10^{-24}$ g, and $\sigma_{\mathrm{prod}}^{\mathrm{fid}}$ is the (process dependent) cross section for muon production at the LHC, within the ATLAS fiducial volume. In this work, we assume a $^{63}_{29}\mathrm{Cu}$ target, which corresponds to $A = 63$ and $\rho_T = 8.96~\mathrm{g/cm^3}$ in Eq. (4). For this analysis, the dominant calorimeter characteristic is the total radiation lengths. Other effects due to the specific detector material are small, and would be taken into account correctly by a full-detector simulation.

We estimate the MFC signal production rate following the schematics in Fig. 1. A muon originating from the IP with momentum p_{in} and direction η interacts at a point x in the material target of length $\ell_T(\eta)$, and produces a MFC, and an outgoing muon of momentum p_{out} which travels in an angle θ relative to the incoming muon direction. The expected number of produced MFCs within the detector acceptance, $\mathcal{A}$ (which includes the MFC target interaction) is[3]

$$N_X = \mathcal{L}_{\mathrm{FT}}^{\mathrm{int}} \sigma_T \int dp_{\mathrm{in}} \int d\eta \, \mathcal{A} \times \mathcal{P}_{\mathrm{in}}(p_{\mathrm{in}}, \eta), \quad (5)$$

where σ_T is the fixed-target MFC production cross section, $\mu T \to \mu T X$, and $\mathcal{P}_{\mathrm{in}}(p_{\mathrm{in}}, \eta)$, is the incoming muon double-differential distribution:

$$\mathcal{P}_{\mathrm{in}}(p_{\mathrm{in}}, \eta) \equiv \frac{1}{\sigma_{\mathrm{prod}}^{\mathrm{fid}}} \frac{d^2 \sigma_{\mathrm{prod}}^{\mathrm{fid}}}{d p_{\mathrm{in}} d\eta}. \quad (6)$$

In addition, below we will be interested in $dN_X/d\rho$, which is straightforward to derive from Eq. (5). For further details on the N_X estimation see the Supplemental Material [26].

B. Signal yields

We use Monte-Carlo (MC) simulations to estimate the signal yield and its ρ distribution. We consider muons from Z and W decays because they provide high-purity muon samples.[4] In the MC sample, events are selected following the criteria in Ref. [27]. In the selected events, only muons in the barrel ($0.1 < |\eta| < 1.05$) are used, since the ID momentum resolution in the barrel is better, and the depth of the calorimeter is approximately constant. In addition, we require a weak ID to MS angular matching requirement of $\theta < 0.1$ to account for the loose IP matching of ME muons.

The incoming muon momentum spectrum, $\mathcal{P}_{\mathrm{fid}}(p_{\mathrm{in}}) \equiv \int d\eta \mathcal{P}_{\mathrm{in}}(p_{\mathrm{in}}, \eta)$, is obtained from a MadGraph5 v2.6.1 simulation [28,29] of the hard process, with up to two additional jets, and interfaced with Pythia 8.230 [30] for showering and hadronization. We apply the MLM jet-matching scheme [31] to combine the different samples, and we use the Delphes 3.4.1 [32] detector simulation with the standard ATLAS card. The momentum spectrum of the selected muons is taken at the truth level of MC generation and smeared based on the published ATLAS muon momentum resolutions ($\sigma_{\mathrm{in}} = 0.015~\mathrm{MeV} + 3 \times 10^{-7} p_{\mathrm{in}}$ and $\sigma_{\mathrm{out}} = 0.05 p_{\mathrm{out}}$, see [25]).

We normalize the muon production rate to match the ATLAS result of $Z \to \mu\mu$ and $W \to \mu\nu$ [27,33,34], and find

$$\sigma_Z^{\mathrm{fid}} = \epsilon_Z^{\mathrm{eff}} \sigma_{pp \to Z \to \mu\mu}^{\mathrm{ATLAS}} = 0.39~\mathrm{nb}, \quad (7)$$

$$\sigma_W^{\mathrm{fid}} = \epsilon_W^{\mathrm{eff}} \sigma_{pp \to W \to \mu\nu}^{\mathrm{ATLAS}} = 3.5~\mathrm{nb}, \quad (8)$$

where $\sigma_{pp \to Z \to \mu\mu}^{\mathrm{ATLAS}}(\sigma_{pp \to W \to \mu\nu}^{\mathrm{ATLAS}}) = 0.78(8.0)~\mathrm{nb}$ [27], and $\epsilon_Z^{\mathrm{eff}}(\epsilon_W^{\mathrm{eff}}) = 0.50(0.44)$ is the efficiency factor relating the ATLAS cuts in Ref. [27] with our selection of the barrel as the fiducial volume. The resulting momentum spectra are shown in Fig. 2.

We note that signal muons may not trigger the combined muon high level trigger. However, Z events can be triggered with high efficiency due to the second muon in the event. In the case of W events with a large energy loss to the mediator particle, it may be challenging to trigger with the

---

[1]The ATLAS calorimeter ranges up to $\Delta x = 144 X_0$, where $X_0 = 1.757$ cm is the radiation length of electrons in iron.

[2]While the calorimeter targets are comprised of various materials, the variation in the event yield is small, and the effect on the experimental sensitivity is negligible.

[3]Note that we have assumed that the detector is cylindrically symmetric, however, ϕ integration can be straightforwardly incorporated to account for possible inhomogeneities.

[4]It would also be interesting to consider other sources of muons at the LHC, e.g., from heavy flavor or J/ψ's decays. There are potentially many more of these muons but they would of course be much more difficult to use for an MFC search due to the large background and lower p_T's.
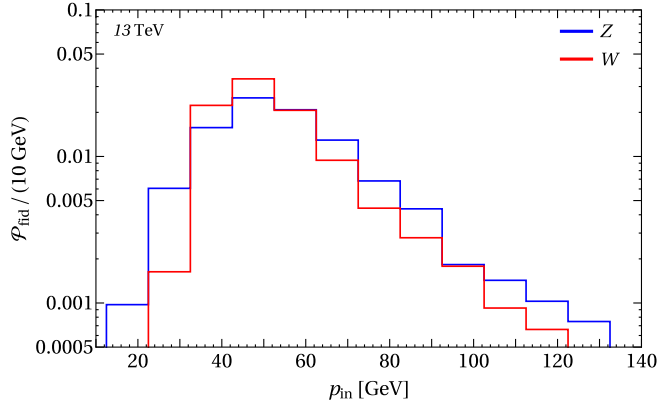
FIG. 2. The differential momentum distributions of muons in our fiducial region, $\mathcal{P}_{\text{fid}}(p_{\text{in}})$, from Z (blue) and W (red) decays. The event selection criteria follow those in [27], The plots are normalized to 1.

single muon trigger by itself or the missing transverse energy (MET) trigger by itself, since the MET at L1 does not take into account the muon momentum. ATLAS has in place trigger tools that allow the collection efficiency to be recovered; in particular, at L1, ATLAS has the L1Topo trigger, where it is possible to lower the p_T thresholds on the MET and the muon in the case of a muon-MET feature. Additionally, in the L1Topo trigger, more complex triggers like an m_T calculation are possible. After the phase-II upgrade of ATLAS, tracking info will be available at the L1 global trigger.

The $\mu T \to \mu T X$ process is simulated in MadGraph 5, including the target nuclear-atomic form factor by modifying the photon-target vertex, see Supplemental Material [26] for details. The Lagrangian of Eq. (1) was implemented as a UFO model [35] by using FeynRules 2.3.32 [36].

The signal ρ distributions $dN_X/d\rho$ are plotted in Fig. 3 for several MFC mass benchmarks. We validate our MC results by comparing them to the Weizsäcker-Williams (WW) approximation [37–39], and find $\mathcal{O}(1)$ agreement, similar to Refs. [40,41].

Finally, combining the above, we estimate that $N_X \sim g_X^2(10^8, 10^7, 10^5)$ for $m_X = 16, 126, 1000$ MeV, respectively, with $X = S$ or V. Thus, for an $\mathcal{O}(1)$ acceptance, and assuming negligible background, we predict that this analysis is sensitive to g_X in the range 10^{-4}–10^{-2}.

C. Backgrounds

The dominant expected background is due to true muons with mismeasured momenta. Motivated by ATLAS results in Ref. [25], we model the momentum mismeasurement with a three Gaussian resolution function, centered at 0. The resolution as a function of ρ is given by

$$\mathcal{R}(\rho) = \frac{1}{N_{\text{SM}}} \frac{dN_{\text{SM}}}{d\rho} = \sum_{i=1,2,3} \frac{c_i}{\sqrt{2\pi\sigma_i^2}} e^{-\frac{\rho^2}{2\sigma_i^2}}, \quad (9)$$
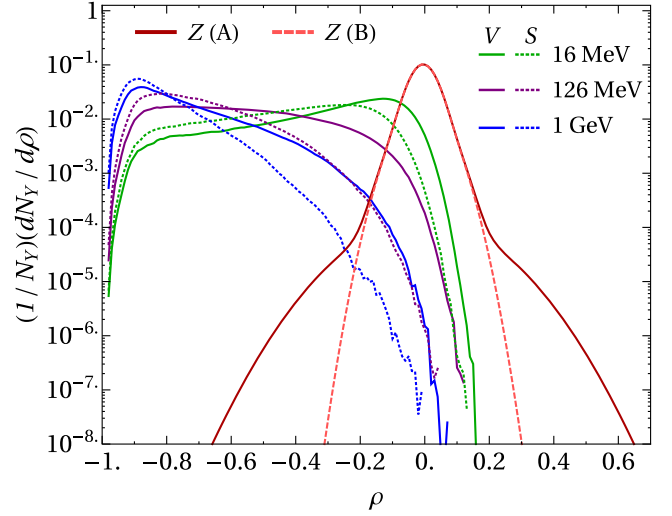

FIG. 3. The ρ distribution, $(1/N_Y)dN_Y/d\rho$, for the SM (background) and MFC, i.e., $Y = SM, S, V$, at different MFC masses.

where $\sigma_1 = 0.035$, $\sigma_2 = 0.057$, $\sigma_3 = 0.15$, $c_1 = 0.75$ and $c_2 = 0.25$. The relative fraction of the third Gaussian is hard to model with the currently available public data. We therefore consider two representative cases

$$c_3^A = 5 \times 10^{-3}, \qquad c_3^B = 0. \quad (10)$$

This resolution function includes hard photon radiation and possible subsequent hadronization effects mentioned in [15] as well as catastrophic energy losses. These effects are well modeled in the full-detector simulation used by the ATLAS based on GEANT [42], as validated by dedicated test-beam campaigns, see e.g., [43,44] and *in situ* [25]. The expected background ρ distributions, $\mathcal{R}$, for each of the above cases are plotted in Fig. 3.

In addition to true muons with mismeasured momenta, there can also be backgrounds from charged pion and kaon decays in-flight. If these decays happen in or near the calorimeter, they can mimic the MFC signal. From publicly available information, we expect that the requirement of dimuon invariant mass to be within 5 GeV of the Z mass reduces these backgrounds to $5:10000$ of the $Z \to \mu\mu$ sample. These backgrounds can be further rejected using an analysis of kink-in-tracks, and calorimeter information. Additionally, since muons from pions decaying in-flight have a minimal momentum fraction of 0.57 of the pion momentum, their contribution at ρ close to -1 is small. We estimate that the in-flight decay background can be rejected to a level between 10^{-7} and 10^{-8}, and it is expected to be subdominant. The ρ distributions and overall normalization for pion and kaon decays can be extracted from a control sample with a same-charge requirement on the tag and probe particles.

D. Reach for MFC

We estimate the sensitivity of the proposed analysis to probe MFCs by a $dN_X/d\rho$ line shape analysis.
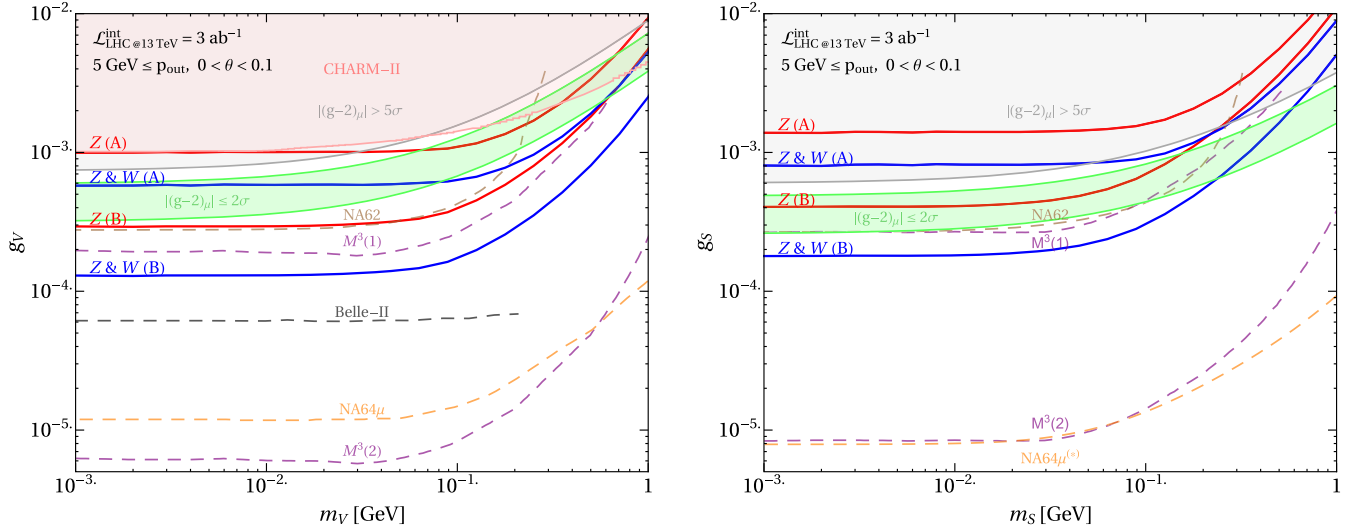
FIG. 4.   The projections of the proposed ATLAS fixed-target-like analysis to probe MFC at the HL-LHC comparing to current constraints from $(g-2)_\mu$ [5,6] and CHARM-II [22,23] as well as to the projection of $M^3(1)(M^3(2))$ [15] with $10^{10}(10^{13})\mu$ on-Target, NA62 [17] with 10^{13} K^+, NA64$_\mu$ [16,19] with 5×10^{12} μ on-Target and Belle II [18] with 50 ab^{-1}. Left: vector mediator; right: scalar mediator.

From the binned ρ distribution, we construct a likelihood function, $L(g_X, m_X)$, and assume that the number of observed events is equal to the expected background events per bin. For a given m_X, we estimate the expected 95% confidence level upper bound on g_X for each of the above background scenarios and for two cases: (i) muons only from Z decays; and (ii) muons from both Z and W decays.

The projections are plotted in Fig. 4 and are compared to the present bounds from $(g-2)_\mu$ [5,6] and CHARM-II [22,23] as well as to the projections of M^3 [15], NA62 [17], NA64$_\mu$ [16,19] and Belle II [18]. We can see that the reach for $m_X \to 0$ can be at the level of $g_X \sim 10^{-3}$–few $\times 10^{-4}$ (depending on the background model) by using only muons from Z. For the case of a combined analysis of Z and W muons, the sensitivity can reach the $g_X \sim 10^{-4}$ level. This part of the parameter space is relevant for the $(g-2)_\mu$ anomaly, to thermal freeze-out dark matter scenarios, see e.g., [15], and comparable to other proposals such as M^3 phase 1. Moreover, in the case that X is a $L_\mu - L_\tau$ gauge boson, our proposal probes a $m_X - g_X$ parameter space which may contribute to $N_{\rm eff}$ and possibly reduce the Hubble parameter tension [45]. Finally, it is worth noting that while our sensitivity projections are for the ultimate HL-LHC dataset of 3 ab^{-1}, even with the current dataset ($\sim$150 fb^{-1}) or the expected Run-3 dataset ($\sim$300 fb^{-1}), it should already be possible to probe at least a portion of these interesting regions of parameter space.

V. SUMMARY

We propose a search for NP using the large sample of muons produced at LHC collisions, and ATLAS detector as a fixed-target experiment sensitive to missing muon momentum signatures. In the proposed analysis, the calorimeter serves as a target for muons, and the muon momentum measurements before and after it are compared. In principle, this strategy, of utilizing high energy colliders as fixed target in the second production, can be adopted in future experiments.

We focus on the possibility that a muonic force carrier is produced in the muon-target interaction and subsequently escapes the detector or decays invisibly. The detector signature corresponding to this scenario is of an unaccounted loss of muon momentum in the calorimeter. The expected sensitivity of the ATLAS experiment to this signature using muons from Z and W decays is comparable to other proposed experiments, and overlaps the parameter space that can explain the observations in the anomalous magnetic dipole moment of the muon.

[1] B. Batell, N. Lange, D. McKeen, M. Pospelov, and A. Ritz, Muon anomalous magnetic moment through the leptonic Higgs portal, Phys. Rev. D **95,** 075003 (2017).

[2] C.-Y. Chen, M. Pospelov, and Y.-M. Zhong, Muon beam experiments to probe the dark sector, Phys. Rev. D **95,** 115005 (2017).

[3] B. Batell, A. Freitas, A. Ismail, and D. Mckeen, Flavor-specific scalar mediators, Phys. Rev. D **98,** 055026 (2018).

[4] L. Marsicano, M. Battaglieri, A. Celentano, R. De Vita, and Y.-M. Zhong, Probing leptophilic dark sectors at electron beam-dump facilities, Phys. Rev. D **98,** 115022 (2018).

[5] G. W. Bennett et al. (Muon g-2 Collaboration), Final report of the Muon E821 anomalous magnetic moment measurement at BNL, Phys. Rev. D **73,** 072003 (2006).

[6] J. Beringer et al. (Particle Data Group Collaboration), Review of particle physics (RPP), Phys. Rev. D **86,** 010001 (2012).

[7] R. Pohl, R. Gilman, G. A. Miller, and K. Pachucki, Muonic hydrogen and the proton radius puzzle, Annu. Rev. Nucl. Part. Sci. **63,** 175 (2013).

[8] R. J. Hill and G. Paz, Nucleon spin-averaged forward virtual Compton tensor at large Q^2, Phys. Rev. D **95,** 094017 (2017).

[9] J. Alexander et al., Dark Sectors 2016 Workshop: Community Report, 2016, http://lss.fnal.gov/archive/2016/conf/fermilab-conf-16-421.pdf.

[10] M. Battaglieri et al., US cosmic visions: New ideas in dark matter 2017: Community report, in U.S. Cosmic Visions: New Ideas in Dark Matter College Park, MD, USA, 2017 (2017), http://lss.fnal.gov/archive/2017/conf/fermilab-conf-17-282-ae-ppd-t.pdf.

[11] J. Beacham et al., Physics beyond colliders at CERN: Beyond the standard model working group report, J. Phys. G **47,** 010501 (2020).

[12] J. P. Lees et al. (BABAR Collaboration), Search for a muonic dark force at BABAR, Phys. Rev. D **94,** 011102 (2016).

[13] M. Chala, U. Egede, and M. Spannowsky, Searching new physics in rare B-meson decays into multiple muons, Eur. Phys. J. C **79,** 431 (2019).

[14] S. N. Gninenko, N. V. Krasnikov, and V. A. Matveev, Muon g-2 and searches for a new leptophobic sub-GeV dark boson in a missing-energy experiment at CERN, Phys. Rev. D **91,** 095015 (2015).

[15] Y. Kahn, G. Krnjaic, N. Tran, and A. Whitbeck, M³: A new muon missing momentum experiment to probe $(g-2)_\mu$ and dark matter at Fermilab, J. High Energy Phys. 09 (2018) 153.

[16] C.-Y. Chen, J. Kozaczuk, and Y.-M. Zhong, Exploring leptophilic dark matter with NA64-μ, J. High Energy Phys. 10 (2018) 154.

[17] G. Krnjaic, G. Marques-Tavares, D. Redigolo, and K. Tobioka, Probing muonic forces and dark matter at kaon factories, arXiv:1902.07715 [Phys. Rev. Lett (to be published)].

[18] Y. Jho, Y. Kwon, S. C. Park, and P.-Y. Tseng, Search for muon-philic new light gauge boson at Belle II, J. High Energy Phys. 10 (2019) 168.

[19] S. N. Gninenko, D. V. Kirpichnikov, M. M. Kirsanov, and N. V. Krasnikov, Combined search for light dark matter with electron and muon beams at NA64, Phys. Lett. B **796,** 117 (2019).

[20] J. Grange et al. (Muon g-2 Collaboration), Muon (g-2) technical design report, arXiv:1501.06858.

[21] X.-G. He, G. C. Joshi, H. Lew, and R. R. Volkas, Simplest Z-prime model, Phys. Rev. D **44,** 2118 (1991).

[22] D. Geiregat et al. (CHARM-II Collaboration), First observation of neutrino trident production, Phys. Lett. B **245,** 271 (1990).

[23] W. Altmannshofer, S. Gori, M. Pospelov, and I. Yavin, Neutrino Trident Production: A Powerful Probe of New Physics with Neutrino Beams, Phys. Rev. Lett. **113,** 091801 (2014).

[24] F. Jegerlehner and A. Nyffeler, The Muon g-2, Phys. Rep. **477,** 1 (2009).

[25] G. Aad et al. (ATLAS Collaboration), Muon reconstruction performance of the ATLAS detector in proton-proton collision data at $\sqrt{s} = 13$ TeV, Eur. Phys. J. C **76,** 292 (2016).

[26] See Supplemental Material at http://link.aps.org/supplemental/10.1103/PhysRevD.101.011701 for details about the signal yields and the muon target cross section calculations.

[27] G. Aad et al. (ATLAS Collaboration), Measurement of $W^\pm$ and Z-boson production cross sections in pp collisions at $\sqrt{s} = 13$ TeV with the ATLAS detector, Phys. Lett. B **759,** 601 (2016).

[28] J. Alwall, R. Frederix, S. Frixione, V. Hirschi, F. Maltoni, O. Mattelaer, H. S. Shao, T. Stelzer, P. Torrielli, and M. Zaro, The automated computation of tree-level and next-to-leading order differential cross sections, and their matching to parton shower simulations, J. High Energy Phys. 07 (2014) 079.

[29] P. de Aquino, W. Link, F. Maltoni, O. Mattelaer, and T. Stelzer, ALOHA: Automatic libraries of helicity amplitudes for feynman diagram computations, Comput. Phys. Commun. **183,** 2254 (2012).

[30] T. Sjostrand, S. Mrenna, and P. Z. Skands, A brief introduction to PYTHIA 8.1, Comput. Phys. Commun. **178,** 852 (2008).

[31] M. L. Mangano, M. Moretti, F. Piccinini, and M. Treccani, Matching matrix elements and shower evolution for top-quark production in hadronic collisions, J. High Energy Phys. 01 (2007) 013.

[32] J. de Favereau, C. Delaere, P. Demin, A. Giammanco, V. Lemaître, A. Mertens, and M. Selvaggi (DELPHES 3 Collaboration), DELPHES 3, A modular framework for fast simulation of a generic collider experiment, J. High Energy Phys. 02 (2014) 057.

[33] M. Aaboud et al. (ATLAS Collaboration), Measurements of the production cross section of a Z boson in association with jets in pp collisions at $\sqrt{s} = 13$ TeV with the ATLAS detector, Eur. Phys. J. C **77,** 361 (2017).

[34] A. M. Sirunyan et al. (CMS Collaboration), Measurement of differential cross sections for Z boson production in association with jets in proton-proton collisions at $\sqrt{s} = 13$ TeV, Eur. Phys. J. C **78,** 965 (2018).

[35] C. Degrande, C. Duhr, B. Fuks, D. Grellscheid, O. Mattelaer, and T. Reiter, UFO—The universal feynrules output, Comput. Phys. Commun. **183,** 1201 (2012).

[36] A. Alloul, N. D. Christensen, C. Degrande, C. Duhr, and B. Fuks, FeynRules 2.0—A complete toolbox for tree-level phenomenology, Comput. Phys. Commun. **185,** 2250 (2014).

[37] K. J. Kim and Y.-S. Tsai, Improved Weizsäcker-Williams method and its application to lepton and *W*-boson pair production, Phys. Rev. D **8,** 3109 (1973).

[38] Y.-S. Tsai, Pair production and bremsstrahlung of charged leptons, Rev. Mod. Phys. **46,** 815 (1974); **49,** 421 (1977).

[39] J. D. Bjorken, R. Essig, P. Schuster, and N. Toro, New fixed-target experiments to search for dark gauge forces, Phys. Rev. D **80,** 075018 (2009).

[40] Y.-S. Liu, D. McKeen, and G. A. Miller, Validity of the Weizsäcker-Williams approximation and the analysis of beam dump experiments: Production of a new scalar boson, Phys. Rev. D **95,** 036010 (2017).

[41] Y.-S. Liu and G. A. Miller, Validity of the Weizsäcker-Williams approximation and the analysis of beam dump experiments: Production of an axion, a dark photon, or a new axial-vector boson, Phys. Rev. D **96,** 016004 (2017).

[42] A. G. Bogdanov, H. Burkhardt, V. N. Ivanchenko, S. R. Kelner, R. P. Kokoulin, M. Maire, A. M. Rybin, and L. Urban, Geant4 simulation of production and interaction of muons, IEEE Trans. Nucl. Sci. **53,** 513 (2006).

[43] P. Amaral *et al.* (ATLAS TileCal Collaboration), A precise measurement of 180-GeV muon energy losses in iron, Eur. Phys. J. C **20,** 487 (2001).

[44] E. L. Berger *et al.* (RD34 Collaboration), A Measurement of the energy loss spectrum of 150-GeV muons in iron, Z. Phys. C **73,** 455 (1997).

[45] M. Escudero, D. Hooper, G. Krnjaic, and M. Pierre, Cosmology with a very light $L_\mu - L_\tau$ gauge boson, J. High Energy Phys. 03 (2019) 071.